Control for Underactuated Reentry Aircraft in Small Angle of Attack

Min Changwan, *Wang Ying*, *Xiao Zhen*, *Dai Shicong*, *Yang Lingxiao*

Science and Technology on Space Physics Laboratory, Beijing 100076, P. R. China

(Received 23 June 2016; revised 2 August 2016; accepted 16 August 2016)

Abstract: The control problem for under-actuated reentry vehicle like HTV-2 is considered with small angle of attack. The control strategy for an aircraft with positive lateral control departure parameter relies on strong lateral stability, which declines with the decrease of the angle of attack. Thus, to control the lateral-directional motion in a stable state is hard and even impossible in some scenarios where the under-actuated reentry vehicle, like HTV-2, flies in a low angle of attack. To address this problem, the lateral-directional open-loop motion characteristics are analyzed. The results show that in an uncontrolled state, the lateral-directional motion can automatically converge to stabilization thanks to the aerodynamic damping effect. Therefore, a method of turning-off the lateral-directional control and inviting aerodynamic damping to control can achieve stability. The six-degree-of-freedom simulation show that the lateral-directional motion can be stabilized by the aerodynamic damping, and the lateral position error caused by the bank angle deviation is limited near the zero-rise angle of attack. The control strategy is effective.

Key words: underactuated reentry vehicle; lateral control deviation parameter; control strategy; small angle of attack; aerodynamic damping

CLC number: V11 **Document code**: A **Article ID**: 1005-1120(2017)06-0593-07

Nomenclature

δ_a	Aileron deflection, per radian
α	Angle-of-attack, radian
β	Sideslip angle, radian.
$\Delta\gamma_v$	Bank angle, radian
C_A	Axis force coefficient
C_N	Normal force coefficient
C_Z^β, $C_Z^{\delta_a}$	Derivative of side force coefficient with respect to sideslip angle and aileron deflection respectively, per radian
C_{lp}, C_{nr}	Roll damp coefficient and yaw damp coefficient, respectively
C_n^β	Derivative of yawing moment coefficient with respect to sideslip angle, per radian
C_l^β	Derivative of rolling moment coefficient with respect to sideslip angle, per radian
$C_n^{\delta_a}$	Derivative of yawing moment coefficient with respect to aileron deflection, per radian
$C_l^{\delta_a}$	Derivative of rolling moment coefficient with respect to aileron deflection, per radian
$C^\beta_{n\_\mathrm{dyn}}$	$C^\beta_{n\_\mathrm{dyn}}=C_n^\beta\cos\alpha+\frac{J_{y1}}{J_{x1}}C_l^\beta\sin\alpha$
LCDP	Lateral control departure parameter
ω_{y1}, ω_{x1}	Yaw and roll angular velocity, radian/s
J_{x1}, J_{y1}	Moments of inertia about x and y body axes respectively, kg·m^2.
J_{x1y1}	Roll-yaw cross product of inertia referred to X_1 and Y_1 axes, kg·m^2
k_{γ_V}, k_{ω_x}, k_β, k_{ω_y}	Aileron-bank angle gain, aileron-roll rates gain, aileron-sideslip angle gain, and aileron-yaw rate gain respectively
$C_n^{\delta_a}$	Derivative of yawing moment coefficient with respect to aileron deflection, per radian
V	Velocity
m	Mass of the aircraft
q	Dynamic pressure, Pa
S, L	Reference area (m^2) and reference length (m), respectively
ω_D	Natural frequency of the Dutch roll mode

* Corresponding author, E-mail address: wy.080808@163.com.

How to cite this article: Min Changwan, Wang Ying, Xiao Zhen, et al. Control for underactuated reentry aircraft in small angle of attack [J]. Trans. Nanjing Univ. Aero. Astro., 2017,34(6):593-599.
http://dx.doi.org/10.16356/j.1005-1120.2017.06.593

0 Introduction

In 1958, Moul and Paulson[1] proposed the parameter LCDP to predict the lateral divergence of controlled vehicle when studying the aerodynamic layout design of a hypersonic glide vehicle. For a long time, LCDP<0[2] has been used as a design guideline to guide aerodynamic layout and control strategy design. This guideline has successfully guided the design of reentry vehicles such as space shuttle[3], *X*-33[4], *X*-37B[5]. With conventional control strategy[6], when LCDP>0, the roll control reverse problem will arise, resulting in lateral-directional instability.

Remote reentry vehicle normally has a wide flight profile. Thus, requiring a negative LCDP in a complete flight mission implies that a directional stabilizer, like ventral fin and tail, or a control mechanism, like rudder, is necessary, but it can be a drawback for the pursing of high performance aircraft.

Among the reentry vehicles already known to the public, the US HTV-2 remote reentry vehicle represents the ultimate coupling design of the aerodynamic and control. Despite its two unsuccessful flight tests, HTV-2 is the aircraft with the most compact aerodynamic shape so far. Ref. [7] presented the general morphology of HTV-2, as shown in Fig. 1. The flat shape of HTV-2 with sharp front and steep sweep has the characteristics of both wave body and lift body[8]. In addition, its rear edge is equipped with an expansion flap (flap rudder) and a reaction control system (RCS) control mechanism.

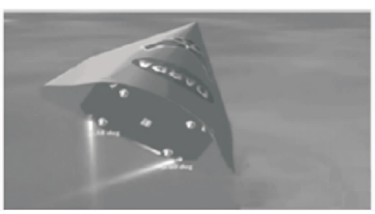

Fig. 1 The configuration of HTV-2

For an aircraft with extremely simple and smooth aerodynamic shape like HTV-2, strong directional static stability is difficult to obtain. Thus the characteristic with a negative LCDP for the whole flight is not easy to achieve. Compared with the strong directional stability, it is easier to obtain strong lateral static stability by adjusting the dihedral or anhedral angle of the body-wing. However, LCDP is easy to be greater than zero with strong lateral static stability. There will be roll "control reverse" problem if the single pair of flap rudder are utilized with conventional control strategy.

In the literature, control measures in the flight state with LCDP>0 have been proposed for space shuttle[9], X-37B[10] and a reusable launch vehicle[11] separately. However, for a minimal-shaped aircraft like HTV-2, these control strategy is rarely effective with LCDP>0. In recent years, Li Huifeng[12-14] carried out relevant work to solve the control problem with LCDP>0, solely relying on the body flap. One of his research is to work out a side-slip angel, which is controlled by ailerons, to dominate the roll channel[12]. He also pointed in other studies[13-14] which stood on the perspective of non-linear system that when LCDP>0, the lateral motion of the controlled aircraft is a non-minimum phase system, therefore he and his team designed a specific controller based on this feature.

Integrated design criteria for aerodynamic and control strategies that match the case of LCDP>0 is provided in Ref. [6]. Therefore, we analyze the problem of the control for small angle of attack and present a solution in this paper.

1 Control Problem Analysis

Here we suppose the lateral-directional motion is controlled by aileron. When LCDP<0, the control law is normally

$$\delta_a = k_{\gamma_V}\Delta\gamma_v + k_{\omega_x}\omega_{x1} \quad k_{\gamma_V} > 0, k_{\omega_x} > 0 \quad (1)$$

When LCDP>0, the control law was proposed in Ref. [6] through lateral-directional single-state feedback stability analysis, as

$$\delta_a = k_{\gamma_V}\Delta\gamma_v + k_{\omega_y}\omega_{y1} \quad k_{\gamma_V} < 0, k_{\omega_y} > 0 \quad (2)$$

Compared with the conventional control law in Eq. (1), the polarity of the feedback gain of the back angle deviation is changed from positive to negative in Eq. (2). The angular velocity feed-

back is changed from the roll angular velocity to the yaw angular velocity. The design constraint of the bank angle deviation feedback gain is shown as

$$\frac{-C_n^{\beta}}{C_n^{\delta_a}}\tan\alpha < k_{\gamma_V} < 0 \tag{3}$$

From the design constraint of k_{γ_V}, it can be seen that as the angle of attack decreases, the range of k_{γ_V} becomes narrower, and when the angle of attack approaches zero, there will be no value for k_{γ_V}. The strategy will fail under a small angle of attack.

The control problem mentioned above can be derived from a physical mechanism as well. For flight states with LCDP>0, the lateral-directional stabilization control, in essence, utilizes C_l^{β} and $C_n^{\delta_a}$, which are the cross-coupling between the lateral and the directional channels. When the bank maneuver is needed, the side slip angle is first generated by the yaw coupling term $C_n^{\delta_a}$, and the rolling moment is produced by the side slip angle through the lateral static stability C_l^{β}. Thus, strong lateral static stability of the aircraft is required in the control mechanism. However, for the aircraft with extremely simple shape like HTV-2, the lateral static stability of it decreases with the decrease of the angle of attack. Fig. 2 shows that when flying at a small angle of attack, the aircraft has poor lateral static stability or even is unstable. Therefore, the strategy using lateral static stability for lateral-directional control will fail because of the poor lateral static stability with small angle of attack, which is consistent with the result of theoretical analysis.

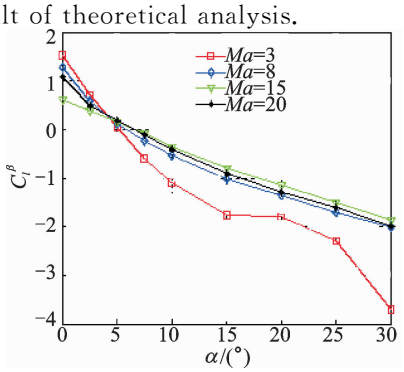

Fig. 2 Lateral static stability versus the angle of attack

2 Open-Loop Stability Analysis

The expression of the lateral-directional state equation is

$$\begin{bmatrix}\Delta\dot{\beta}\\ \Delta\dot{\omega}_{x1}\\ \Delta\dot{\omega}_{y1}\\ \Delta\dot{\gamma}_v\end{bmatrix}=\begin{bmatrix}c_{6\beta} & \sin\alpha & \cos\alpha & c_{10\beta}\\ b_{6g} & b_{1g} & 0 & 0\\ b_{6p} & 0 & b_{2p} & 0\\ 0 & \cos\alpha & -\sin\alpha & 0\end{bmatrix}\cdot\begin{bmatrix}\Delta\beta\\ \Delta\omega_{x1}\\ \Delta\omega_{y1}\\ \Delta\gamma_v\end{bmatrix}+\begin{bmatrix}c_{8\beta}\\ b_{8g}\\ b_{8p}\\ 0\end{bmatrix}\Delta\delta_a \tag{4}$$

where

$$b_{6g}=\frac{J_{x1y1}C_n^{\beta}qSL+J_{y1}C_l^{\beta}qSL}{J_{x1}J_{y1}-J_{x1y1}^2}\approx\frac{C_l^{\beta}qSL}{J_{x1}}$$

$$b_{6p}=\frac{J_{x1y1}C_l^{\beta}qSL+J_{x1}C_n^{\beta}qSL}{J_{x1}J_{y1}-J_{x1y1}^2}\approx\frac{C_n^{\beta}qSL}{J_{y1}}$$

$$b_{8g}=\frac{J_{x1y1}C_n^{\delta_a}qSL+J_{y1}C_l^{\delta_a}qSL}{J_{x1}J_{y1}-J_{x1y1}^2}\approx\frac{C_l^{\delta_a}qSL}{J_{x1}}$$

$$b_{8p}=\frac{J_{x1y1}C_l^{\delta_a}qSL+J_{x1}C_n^{\delta_a}qSL}{J_{x1}J_{y1}-J_{x1y1}^2}\approx\frac{C_n^{\delta_a}qSL}{J_{y1}}$$

$$c_{8\beta}=\frac{C_Z^{\delta_a}qS}{mV}$$

$$c_{6\beta}=\frac{C_Z^{\beta}qS+C_{\mathrm{A}}qS\cos\alpha+C_{\mathrm{N}}qS\sin\alpha}{mV}$$

$$c_{10\beta}=\frac{mg\cos\Theta\cos\gamma_v}{mV}$$

$$b_{1g}=-\frac{J_{y_1}}{J_{x_1}J_{y_1}-J_{x_1y_1}^2}\frac{C_{lp}}{V}qSL^2$$

$$b_{2p}=-\frac{J_{x_1}}{J_{x_1}J_{y_1}-J_{x_1y_1}^2}\frac{C_{nr}}{V}qSL^2$$

The characteristic equation of the open-loop system is derived as

$$\begin{aligned}\Delta=&s^4+(-b_{2p}-c_{6\beta}-b_{1g})s^3+\\&(-b_{6g}\sin\alpha-b_{6p}\cos\alpha+b_{1g}b_{2p}+b_{1g}c_{6\beta}+b_{2p}c_{6\beta})s^2+\\&(b_{2p}b_{6g}\sin\alpha+c_{10\beta}b_{6p}\sin\alpha-b_{1g}b_{2p}c_{6\beta}+\\&b_{1g}b_{6p}\cos\alpha-b_{6g}c_{10\beta}\cos\alpha)s+\\&(b_{2p}b_{6g}c_{10\beta}\cos\alpha-b_{1g}b_{6p}c_{10\beta}\sin\alpha)\end{aligned} \tag{5}$$

The characteristic equation has four characteristic roots. In general, these four characteristic roots are two real roots and one pair of conjugate roots. The two roots correspond to the roll mode and the spiral mode individually, and the conjugate roots correspond to the Dutch roll mode[15].

Scenario I

Regardless of the effect of the aerodynamic

damping terms b_{1g} and b_{2p}, and ignoring the small parameters $c_{6\beta}$ and $c_{10\beta}$, the open-loop system characteristic equation is simplified as

$$\Delta = s^2\left[s^2 + (-b_{6g}\sin\alpha - b_{6p}\cos\alpha)\right] \tag{6}$$

In Eq. (6), the characteristic root of the roll mode and the spiral mode is zero, and the Dutch roll mode corresponds to the conjugate virtual root with zero real part, and the natural oscillation frequency of the Dutch roll is shown as

$$\omega_{\mathrm{D}}^2 = -b_{6g}\sin\alpha - b_{6p}\cos\alpha = -\frac{1}{J_{y_1}}qSL\left(C_n^{\beta}\cos\alpha + \frac{J_{y_1}}{J_{x_1}}C_l^{\beta}\sin\alpha\right) = -\frac{1}{J_{y_1}}qSL\cdot C_{\mathrm{n\_dyn}}^{\beta} \tag{7}$$

Considering the common situation of $C_{n\_\mathrm{dyn}}^{\beta} < 0$, setting the initial yaw angular velocity as 1 °/s and all other states as zero, the response of each system state is shown in Figs. 3—6. The motion pattern of ω_{x1}, ω_{y1} and β is constant amplitude oscillation with frequency equal to ω_D, under the initial angular velocity. But the bank angle is monotonically divergent.

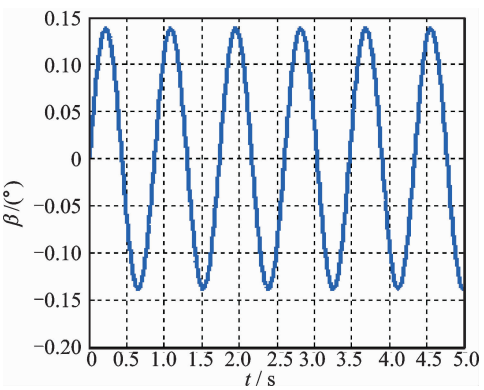

Fig. 3 Response of the side-slip angle

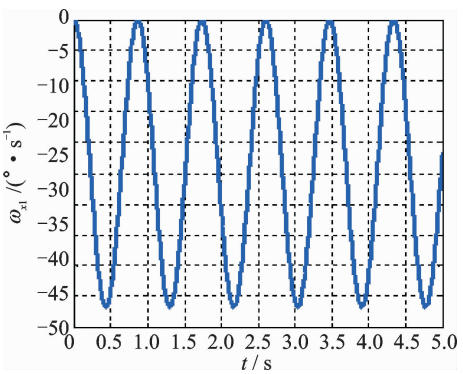

Fig. 4 Response of the roll angular velocity

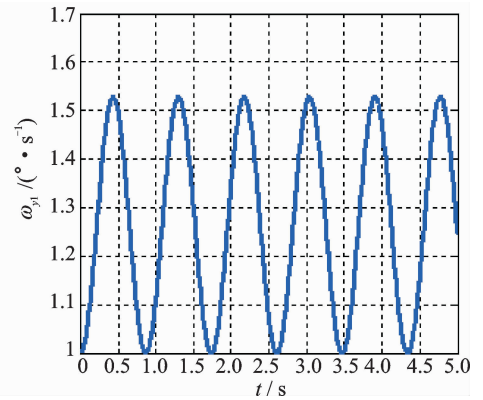

Fig. 5 Response of the yaw angular velocity

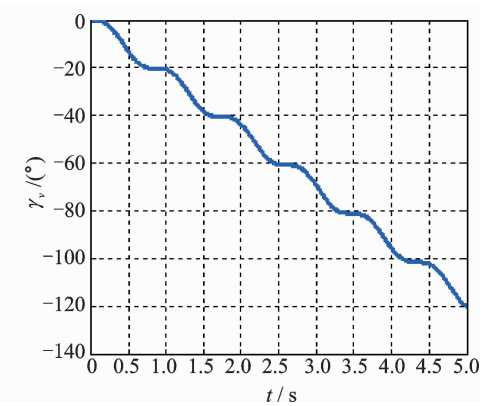

Fig. 6 Response of the bank angle

Scenario II

Next, we consider the effects of aerodynamic damping items b_{1g} and b_{2p} and the small parameters $c_{6\beta}$ and $c_{10\beta}$. According to the final value theorem, the expression of the final value of the system states are derived in Eq. 8 with any initial disturbance. It can be seen that the final value of each state of the open-loop system converges to zero at any initial interference

$$\lim_{t\to\infty}\boldsymbol{X}(t) = \lim_{s\to 0}s(s\boldsymbol{I}-\boldsymbol{A})^{-1}\boldsymbol{X}(0) = \begin{bmatrix}0&0&0&0\\0&0&0&0\\0&0&0&0\\0&0&0&0\end{bmatrix}\boldsymbol{X}(0) \tag{8}$$

With the same initial disturbance as Scenario I presented, the response of each state of the system is shown in Figs. 7—10. ω_{x1}, ω_{y1} and β converge with oscillation quickly. The bank angle appears to diverge slowly at the beginning but eventually converges to zero and the convergence process is slower.

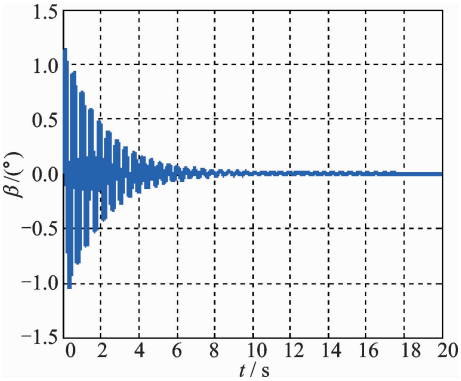

Fig. 7 Response of the side-slip angle

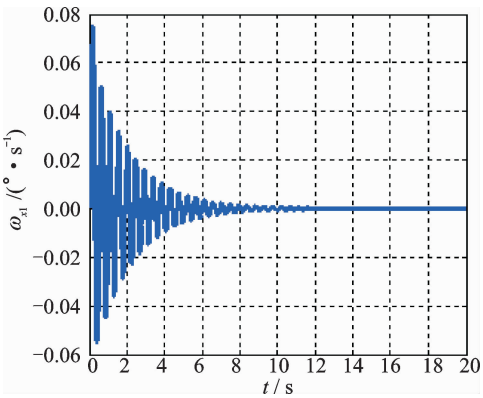

Fig. 8 Response of the roll angular velocity

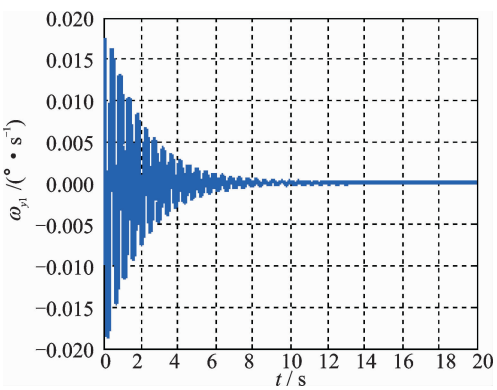

Fig. 9 Response of the yaw angular velocity

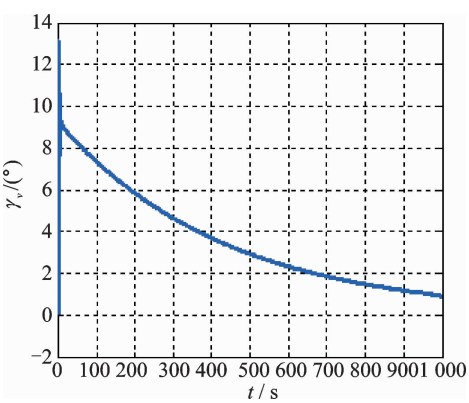

Fig. 10 Response of the bank angle

In the typical state, the change of b_{1g}, b_{2p}, $c_{6\beta}$ and $c_{10\beta}$ with the Mach number is shown in Fig. 11. In the high Mach state, the aerodynamic damping effect is weak. Thus, the effect of aerodynamic damping on the motion of the system can be neglected. With the decrease of the number of Mach, the aerodynamic damping effect is enhanced. There is a possibility for the uncontrolled aircraft to converge in the effect of aerodynamic damping.

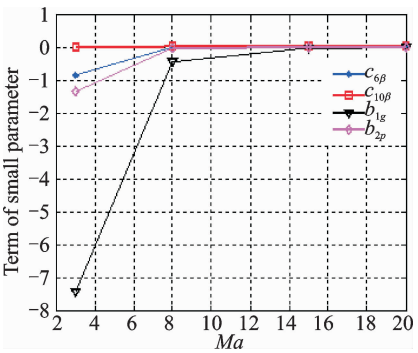

Fig. 11 Change of typical parameter with the Mach number

3 Simulation Analysis

For the long-range reentry vehicles, the small angle of attack often occurs in the low Mach state for a short period of time before landing, as shown in Fig. 10 where the lateral-directional aerodynamic damping effect is enhanced in the low Mach state. When the aircraft flies with small angle of attack and can not be stabilized based on the design criteria of LCDP>0, the use of aerodynamic damping to achieve lateral-directional angular velocity stability can be considered.

Based on the above strategy, six degrees of freedom simulation is carried out. Considering the uncertainty of the parameters, the simulation curves are shown in Fig. 12. At the end of flight, the lateral static stability decreases as the angle of attack decreases, the polarity of the LCDP changes from positive to negative, the control strategy based on the LCDP>0 will be invalidated.

When the value of LCDP reaches the critical point, the control to the lateral-directional is released, and the lateral-directional angular velocity

and side slip angle can be stabilized by aerodynamic damping. In a short time, the bank angle deviation shows an increasing trend, but the error is small. At the same time, near the zero-lift angle of attack, lift is relatively small. Under the combined effect, the lateral position error caused by the bank angle is small, the effectiveness of the strategy is verified.

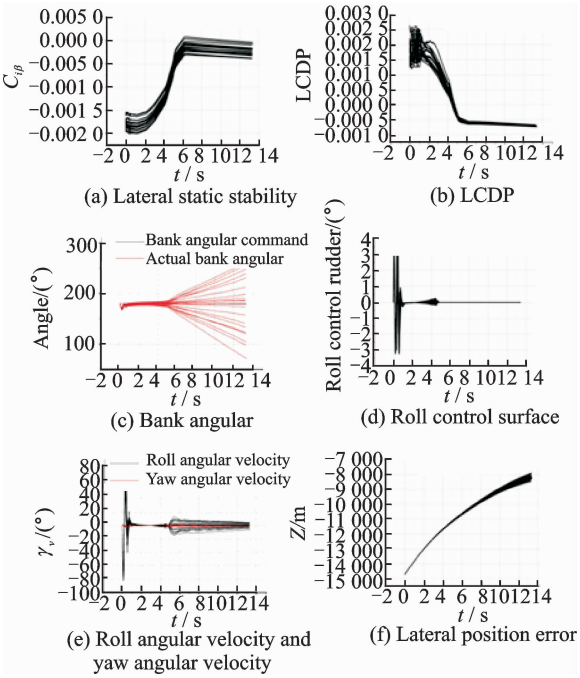

Fig. 12 Simulation analysis curve

4 Conclusions

A flight control strategy for underactuated reentry aircraft in small angle of attack is investigated, in which a control strategy using aerodynamic damping is proposed to stabilize the system. The simulation results show that the attitude of the system can be stabilized and the guidance error is small.

The control strategy proposed in this paper requires knowledge of LCDP in flight to trigger switch of control strategy. However, how to obtain the value of LCDP in flight need further research in future.

References:

[1] MOUL M T, PAULSON J. Dynamic lateral behavior of high performance aircraft [R]. NACA RML58EE. 1958.

[2] ZHU L G, WANG Y F, ZHUANG F G, et al. Lateral-directional departure criteria analysis of high-speed and high maneuverability aircraft [J]. Journal of Astronautics, 2006, 28(6):1550-1553.

[3] RICHARD E D. Coupling dynamics in aircraft:A historical perspective [R]. NASA Special Publication, 1997-532,1997.

[4] THOMPSON R A. Review of X-33 hypersonic aerodynamic and aerothermodynamics development[C]// International Congress of Aeronautical Science. Harrogate, United Kindom:Optimage.

[5] CHAUDHARY A, NGUYEN V, TRAN H. Dynamics and stability and control characteristics of the X—37[R]. AIAA 2001-4383,2001:1-10.

[6] WANG Y,MIN C W, LIU X M,et al. Study on lateral-directional stable design of HTV-2 like vehicle [J]. Journal of Astronautics, 2017, 38(6):583-589.

[7] ZHEN H P, JIANG C W. Review of hypersonic technology test vehicle HTV-2 [J]. Aerodynamic Missile Journal, 2013(6):7-13.

[8] GAO Q, ZHAO J B, LI Q. Study on lateral-directional stability of HTV-2 like configuration [J]. Journal of Astronautics, 2014, 35(6):657-662.

[9] KAER G C. Space shuttle entry/landing flight control design description [C]//AIAA Guidance and Control Conference. San Diego, USA:[s. n.], 1982: 1-12.

[10] LEE H P, CHANG M, KAISER M K. Flight dynamics and stability and control characteristics of X-33 technology demonstrator vehicle [R]. AIAA 1998-4410,1998.

[11] WU L N, HUANG Y M, HE CH L. Reusable launch vehicle lateral control design of glide return phase [J]. Journal of Nanjing University of Aeronautics &Astronautics,2009, 41(3):329-333. (in Chinese)

[12] SHI L N, LI H F, ZHANG R. Gliding reentry vehicle lateral/directional coupling attitude control strategy. [J]. Journal of Beijing University of Aeronautics and Astronautics, 2016, 42(1): 120-129. (in Chinese)

[13] WANG Z H, LI H F, BAO W M. Body-flap attitude control method for a lifting reentry vehicle [J]. Journal of Beijing University of Aeronautics and Astronautics, 2015,41(1): 1-10. (in Chinese)

[14] SUN S H, ZHANG R, LI H F. Cascade attitude

control for nonminimum phase lifting reentry vehicles [J]. Journal of Astronautics, 2017, 38(1):41-49.

[15] NELSON R C. Flight stability and automatic control [M]. Second Edition. Beijing: National Defense Industry Press, 2008:199-209.

Prof. **Min Changwan** received his B. S. and Ph. D. degrees in the Design of Vehicle from Northwestern Polytechnical University, Xi′an, China, in 1993 and 1999, respectively. In 1999, he joined the Science and Technology on Space Physics Laboratory. His research is focused on the design of vehicle.

Ms. **Wang Ying** received her B. S. degree in Automation from Yan Shan University in 2007 and Master′s degree in Navigation Guidance and Control from Beijing Institute of Technology in 2009. She joined the Science and Technology on Space Physics Laboratory in July 2009 as a designer. Her research is focused on the attitude control of the aircraft.

Dr. **Xiao Zhen** received his B. S. and Ph. D. degrees in Navigation Guidance and Control from Beihang University, Beijing, China, in 2003 and 2008, respectively. In 2008, he joined the Science and Technology on Space Physics Laboratory. His research is focused on the design of Vehicle.

Mr. **Dai Shicong** received his Ph. D. degree in Navigation Guidance and Control from Beihang University, Beijing, China, in 2016. In 2016, he joined the Science and Technology on Space Physics Laboratory. His research is focused on the flight control.

Ms. **Yang Lingxiao** received his B. S. degree in Automation from Harbin Institute of Technology University in 2013 and Master of Engineering degree in Design of Vehicle from CASC in 2016. She joined the Science and Technology on Space Physics Laboratory in July 2016 as a designer. Her research is focused on the optimization of flight path.

(Executive Editor: Zhang Bei)